nature chemistry

ARTICLES

PUBLISHED ONLINE: 22 SEPTEMBER 2013 | DOI: 10.1038/NCHEM.1757

Water vibrations have strongly mixed intra- and intermolecular character

Krupa Ramasesha[†‡], Luigi De Marco[‡], Aritra Mandal and Andrei Tokmakoff[†*]

The ability of liquid water to dissipate energy efficiently through ultrafast vibrational relaxation plays a key role in the stabilization of reactive intermediates and the outcome of aqueous chemical reactions. The vibrational couplings that govern energy relaxation in H_2O remain difficult to characterize because of the limitations of current methods to visualize inter- and intramolecular motions simultaneously. Using a new sub-70 fs broadband mid-infrared source, we performed two-dimensional infrared, transient absorption and polarization anisotropy spectroscopy of H_2O by exciting the OH stretching transition and characterizing the response from 1,350 cm^{-1} to 4,000 cm^{-1}. These spectra reveal vibrational transitions at all frequencies simultaneous to the excitation, including pronounced cross-peaks to the bend vibration and a continuum of induced absorptions to combination bands that are not present in linear spectra. These observations provide evidence for strong mixing of inter- and intramolecular vibrations in liquid H_2O, and illustrate the shortcomings of traditional relaxation models.

Most chemical reactions in nature happen under aqueous conditions, in which the ultrafast motions of liquid water play a crucial role in activating reactants and stabilizing reactive intermediates. Solutes dissolved in water are influenced greatly by the vibrational motions of the surrounding water, which include their internal bond vibrations and the orientational and translational motions. Unlike other liquids, water's intermolecular motions span an enormous range of frequencies, making vibrational energy relaxation in liquid H_2O a particularly complex interplay between intra- and intermolecular relaxation pathways that is influenced by anharmonic vibrational coupling, hydrogen-bonding interactions and dielectric fluctuations. The timescales and pathways for the relaxation of vibrational excitation in H_2O are the subject of numerous recent experimental[1–11] and theoretical[12–17] investigations. Most of these studies discuss relaxation processes in the weak coupling regime, which effectively allows the contributions from stretching, bending and intermolecular modes to evolve independently. This leads to cascading downhill energy relaxation through intramolecular vibrations and into the low-frequency intermolecular modes. This picture persists even though recent studies established that the OH stretching vibration of water cannot be described simply as local bond stretching or symmetric/asymmetric vibrations, but as a collective excitation of several molecules[15–17]. Here we present ultrafast broadband infrared spectra of H_2O that provide evidence for the strongly mixed character of all intra- and intermolecular vibrations and non-adiabatic vibrational dynamics in water.

As displayed in Fig. 1a, the molecular vibrational motions of liquid water contribute to mid-infrared absorption features that span a wide range of frequencies, including the OH stretch vibration centred at 3,400 cm^{-1}, the H_2O bend vibration centred at 1,650 cm^{-1}, intermolecular vibrations such as librations (hindered rotations) between 700 cm^{-1} and 400 cm^{-1}, and hydrogen-bond stretching and deformation at even lower frequencies. To investigate properly the couplings and energy transfer between these vibrations therefore requires an experimental technique that can probe the entire mid-infrared spectrum with high time-resolution. Until now, experiments have been limited either by insufficient time resolution or by limited spectral bandwidth. To investigate vibrational dynamics in water, we used a new femtosecond laser plasma source that generates mid-infrared pulses with a bandwidth many times that of traditional optical parametric amplifiers (OPAs) and a pulse duration of $<$70 fs. The spectrum of the broadband probe is shown in green in Fig. 1a. We used these pulses to perform broadband transient absorption and two-dimensional infrared (2D IR) spectroscopy on water in which the OH stretch vibration of H_2O was excited in the 3,100–3,700 cm^{-1} region using the pump spectrum shown in blue in Fig. 1a, and the region between 1,350 cm^{-1} and 4,000 cm^{-1} was probed. 2D IR measurements allow us to observe vibrational couplings of the OH stretch vibration with other degrees of freedom, and frequency-dispersed transient absorption experiments monitor vibrational and orientational relaxation processes.

Results and discussion

Transient infrared spectra and spectral assignments. Figure 1b,c displays the broadband transient absorption and 2D IR spectra of H_2O at waiting times of 100 fs and 50 fs, respectively. A 2D IR spectrum is the change in absorption on exciting a vibration of frequency ω_1 and detecting it at ω_3 after a waiting time τ_2. The transient absorption at a given waiting time is a projection of this surface onto ω_3. Both spectra exhibit cross-peak bleaches (blue) and induced absorptions (red) from the excited OH stretch vibration to a continuum of overtone and combination bands. The 2D IR and the transient absorption spectra are dominated by a bleach at the OH stretch frequency ($\omega_3 = 3{,}400$ cm^{-1}), and a broad induced absorption at lower frequencies. The diagonal region bears some similarity to results obtained with narrower bandwidth pulses[6,9], but the off-diagonal region reveals far more extensive vibrational couplings. On OH stretch excitation, we also see the immediate appearance of a bleach cross-peak with the water bending transitions at $\omega_1 = 3{,}400$ cm^{-1} and $\omega_3 = 1{,}680$ cm^{-1}.

Department of Chemistry, Massachusetts Institute of Technology, Cambridge, Massachusetts 02139, USA; [†]Present addresses: Department of Chemistry, University of California-Berkeley, Berkeley, California 94720, USA (K.R.); Department of Chemistry, University of Chicago, Chicago, Illinois 60637, USA (A.T.); [‡]These authors contributed equally to this work. *e-mail: tokmakoff@uchicago.edu

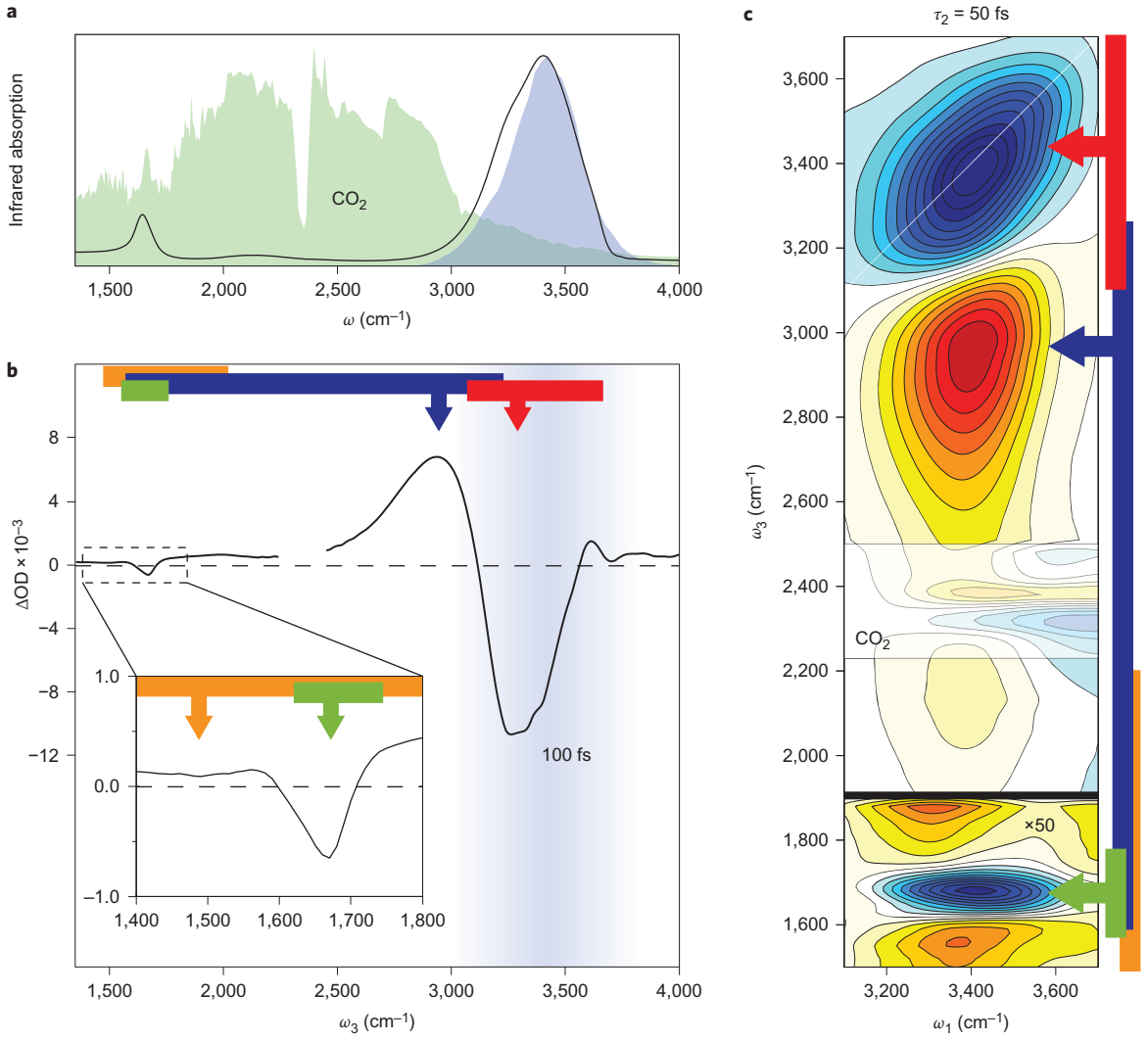

Figure 1 | Steady-state and transient infrared spectra of liquid H_2O. a, Infrared absorption spectrum of liquid H_2O (black) shows transitions across the mid-infrared region. Spectra of the 3,400 cm^{-1} pump and the broadband infrared probe pulse are overlaid in blue and green, respectively. **b**, Broadband transient absorption spectrum of H_2O at $\tau_2 = 100$ fs after the pump. The inset shows an enlargement of the bend region to emphasize a 35 cm^{-1} blue shift of the bleach relative to the bend peak in the infrared spectrum. **c**, Broadband 2D IR spectrum of H_2O at $\tau_2 = 50$ fs shows the diagonal axis as a white line, the cross-peak ridge that stretches vertically across the entire detected frequency region and the cross-peak to the bend vibration. For both **b** and **c**, bleaches refer to negative change in absorption and induced absorptions are positive. Colour-coded bars represent transitions illustrated in Fig. 2b (red, bleach of stretch; blue, induced absorption; green, bleach of bend; orange, induced absorption). The region near 2,300 cm^{-1} is shaded to cover distortions caused by atmospheric CO_2.

This is consistent with the anharmonic couplings reported in pump–bend/probe–stretch experiments[2]. The presence of cross-peaks in a 2D IR spectrum as early as 50 fs indicates that the coupling of these vibrations is strong enough that the nature of the vibrational eigenstates is fundamentally altered, which leads to a mixed bend–stretch character. Such a coupling indicates that the normal modes of the molecule are a poor representation of the true vibrational eigenstates. Also, the bleach of the bend in 2D IR and transient absorption spectra is blue shifted by 35 cm^{-1} from its equilibrium value (Fig. 1b, inset), which suggests that the bend–stretch coupling is stronger for water molecules with higher bending frequencies.

The bend cross-peak bleach is superimposed on an induced absorption ridge that stretches continuously from $\omega_3 > 3{,}200$ cm^{-1} to frequencies below our detection limit of 1,350 cm^{-1}. The induced absorption is particularly striking because it peaks at $\omega_3 = 2{,}950$ cm^{-1}, 450 cm^{-1} below the corresponding bleach, and such a frequency shift is unphysically large to be a simple OH anharmonic shift. Also, the induced absorption is qualitatively different from the transient OH stretching spectrum observed after pumping the H_2O bend[2]. These induced absorptions represent vibrational states that can only be accessed by two sequential mid-infrared photons with energies in the range 3,200–3,600 cm^{-1} and 2,600–3,000 cm^{-1}, respectively (Fig. 2b). However, the one-photon absorption spectrum (Fig. 2c) is clear in the corresponding 6,000–6,400 cm^{-1} region[18]. Therefore, this band is not an overtone or combination band (Fig. 2a), but reflects an excitation-induced effect absent in a one-photon measurement.

Rapid and efficient intermolecular transfer of OH vibrational excitation has been described in recent experiments and theory. In some cases, this process is attributed to resonance-energy transfer, a weak interaction between donor and acceptor that results in energy transfer without memory[19]. In other cases, the OH stretch is described as a delocalized vibration, or vibrational exciton, that involves coherent motion spanning 1–6 water molecules[15–17]. Also

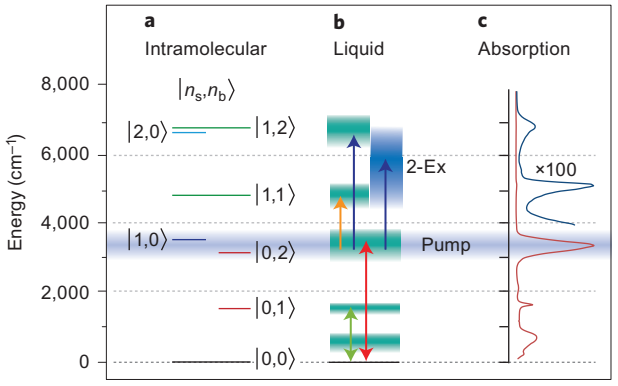

Figure 2 | Vibrational states and energy levels for molecular and liquid H_2O. a,**b** Intramolecular (**a**) and liquid (**b**) energy level diagrams of H_2O representative of the bend–stretch coupling and vibrational delocalization pictures, respectively. The arrows in **b** illustrate transitions observed in the experiments and are colour-coded to match Fig. 1b,c. The shaded bar illustrates the excitation frequencies. In **a**, $|n_s,n_b\rangle$ refers to internal states (n_s refers to the stretch quantum number and n_b refers to the bend quantum number). In **b**, the two-exciton manifold (2-Ex) is represented in blue. **c**, Comparison of the near, mid- and far-infrared absorption spectra of liquid H_2O from 10 cm^{-1} to 8,000 cm^{-1} (ref. 18).

here, an OH transition dipole interaction was used to describe the coupling. Explicit modelling of 2D IR spectra with such exciton models captures the width of the OH excitation in ω_1, but does not reproduce the induced absorption features in ω_3. Therefore, our data are not described by resonant energy transfer or transition dipole coupling, which are linear couplings based on the energy splitting between donor and acceptor states and the magnitude of their transition dipoles. Instead, the broad induced absorptions in our experiments demonstrate that excitation of the OH stretch massively alters the energy of the doubly excited states of the coupled system, which requires a strong nonlinear or anharmonic coupling between exciton states. Excitation of one OH exciton couples strongly enough to other OH excitons that subsequent excitation to a doubly excited state can occur at a much lower energy, as shown in Fig. 2b. Such interactions are not entirely surprising when we discuss the band structure of the OH stretch and recognize that these collective excitations are delocalized over shared subsets of molecules, and differ by the vibrational phase relationships between oscillators. This excitation-induced shift is analogous to the frequency shift in electronic systems attributed to the biexciton binding energy.

In addition to delocalization of the OH stretch vibration, there is evidence of strong stretch–bend coupling. On forming hydrogen bonds in water, the frequency of the OH stretch red-shifts whereas the bend frequency blue-shifts. These effects shift the OH oscillator towards resonance with the bending overtone transition, which results in a Fermi resonance between the $v=1$ level for hydrogen-bonded OH oscillators and the $v=2$ state of the bending mode. Evidence of this Fermi resonance was observed recently in broadband 2D IR spectra of HOD in D_2O (ref. 20). Therefore the broad bleach at 3,400 cm^{-1} spanning over 500 cm^{-1} is probably caused by contributions from both stretch and bend overtone excitations, and the bleach and induced absorption in the 3 μm region does not report directly on the anharmonicity of a single OH stretch vibration. These findings also argue that the stretch–bend Fermi resonance is involved in the debated residual structure at 3,250 cm^{-1} in the infrared absorption and Raman spectra of H_2O.

Although a clear bleach of the bend fundamental transition is present, there is no clear induced absorption attributable to a distinct stretch–bend combination band. Rather, a broad background appears that is not discernible from the stretch induced absorption. Stretch anharmonicity leads to near-degeneracy between the $|2,0\rangle$ and $|1,2\rangle$ vibrations, as shown in Fig. 2a where the states are represented as $|n_s,n_b\rangle$, n_s refers to the stretch quantum number and n_b refers to the bend quantum number. This near-degeneracy ensures that these states will be mixed strongly by the intermolecular fluctuations that modulate their energy about the degeneracy point. As a result, the mixing of bend and stretch is strong enough that their vibrational character is intertwined inextricably, and is influenced strongly by the intermolecular motions that determine the fate of this interaction. Therefore, we believe that the intrinsic vibrational excitations in H_2O are highly mixed and include contributions from the OH stretch, the H_2O bend and the intermolecular vibrations.

Ultrafast energy relaxation. With these spectral assignments in hand, we examined the waiting-time dependence of the 2D IR and transient absorption spectra to describe the dynamics of these vibrational excitons. Figure 3a shows a series of 2D IR spectra of H_2O at different waiting times, and the waiting-time-dependent broadband dispersed transient absorption spectra are displayed in Fig. 3b. The induced absorption relaxes on a 250 fs timescale in the broadband 2D IR spectra across all frequencies, consistent with the timescale observed by narrowband experiments within the stretch and bend windows[3]. The 2D IR spectra show a fast loss of frequency correlation in the OH stretch region with a timescale of 176 ± 39 fs (Fig. 4c), as seen from the evolution of the centre line slope of the bleach, centred at 3,400 cm^{-1}. The centre line slope does not display a strong dependence on frequency.

Our observations qualitatively differ from previous 2D IR measurements with narrower spectral bandwidths, in which 2D IR surfaces showed a loss of frequency correlation within 50 fs and the decay of the induced absorption at $\omega_3 = 3{,}000$ cm^{-1} in less than 100 fs (refs 6,9). Previous measurements also showed a ~300 cm^{-1} splitting between the bleach and induced absorption peaks compared to our ~450 cm^{-1}, which illustrates that the location and breadth of spectral features are sensitive to the spectral characteristics of the excitation and probing pulses[6,9]. 2D IR spectra calculated from theoretical exciton models show an inhomogeneously broadened doublet with a 300 cm^{-1} splitting between bleach and induced absorption[13,16]. The calculated induced absorption extends to ~2,800 cm^{-1} (ref. 13), but does not include the extended ridge seen in our experiment.

Transient absorption spectra were analysed with singular value decomposition (SVD) between 100 fs and 5,000 fs to determine distinct characteristic timescales and spectral features in the data. This analysis confirms that after 100 fs, relaxation can be described in terms of the two spectral components shown in Fig. 4a, the time components of which are displayed in Fig. 4d. The first component yielded a spectrum that we constrain to match the longest time spectrum, and is characterized by a 720 fs rise timescale. The second component resembles the early time spectrum and consists of the continuum response that decayed with a timescale of 275 fs. Although the minimum of the 3,400 cm^{-1} bleach appears to red shift with time, also seen in the diagonal peak in the 2D IR spectrum, SVD suggests that the spectrum is composed primarily of two components, the early time spectrum and the long time spectrum. The 720 fs SVD component spectrum is quantitatively identical to a 3° thermal difference infrared spectrum.

This apparent spectral shifting effect has been observed in the OH stretching range before and our data show that it spans the entire mid-infrared region. Owing to the correlation with the thermal difference spectrum, the spectral shifting has been ascribed to 'heating' of the liquid, in which energy transfer to intermolecular motions leads to a net weakening of hydrogen bonds[21]. However, we

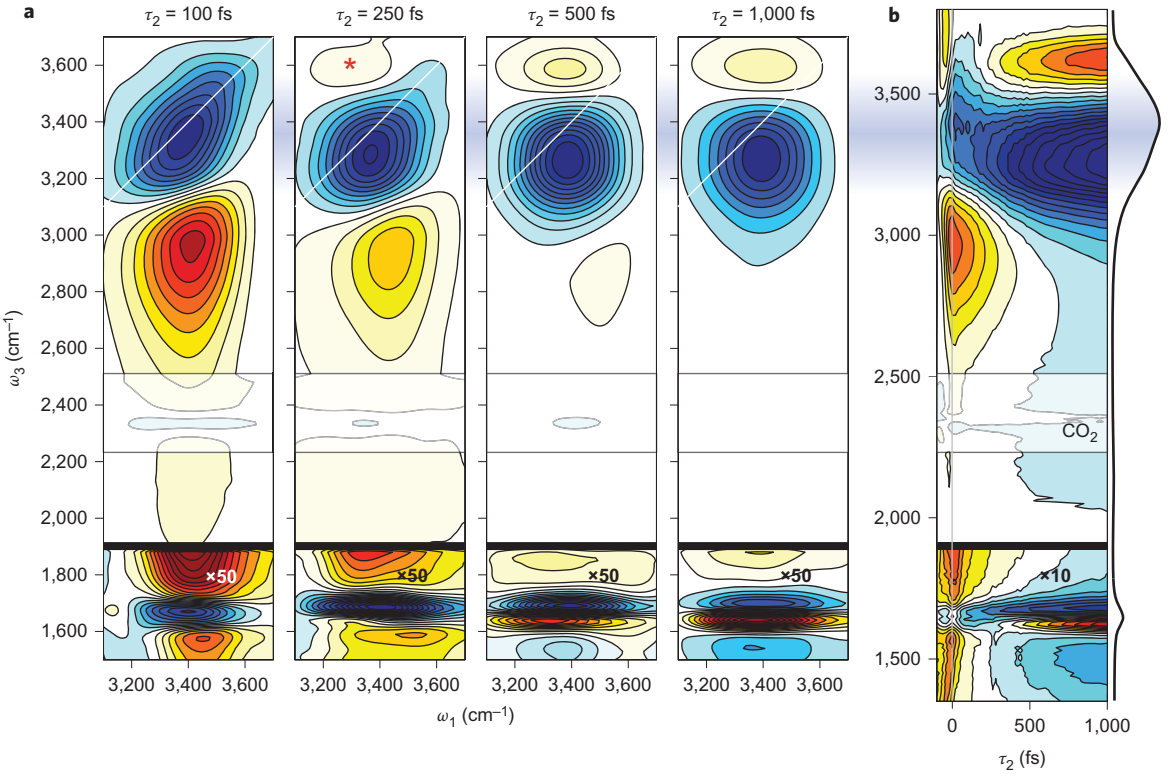

Figure 3 | Broadband 2D IR and transient absorption spectra of H_2O as a function of waiting time between excitation and probing. a, Broadband 2D IR spectra at waiting times of $\tau_2 = 100$ fs, 250 fs, 500 fs and 1 ps show the evolution of the shape of the feature at 3,400 cm^{-1} and the appearance of the long time spectrum at short waiting times. The spectra are individually normalized to their minima. For $\omega_3 < 2{,}000$ cm^{-1}, spectra are magnified by a factor of 50. The red asterisk on the $\tau_2 = 250$ fs spectrum highlights the $(\omega_1, \omega_3) = (3{,}200, 3{,}600)$ cm^{-1} feature discussed in the text. **b**, Broadband dispersed transient absorption spectrum of H_2O taken under magic-angle polarization conditions. The Fourier transform infrared spectrum of H_2O is aligned with the ω_3 axis to guide the eye. The feature at $\omega_3 \approx 2{,}300$ cm^{-1} results from atmospheric CO_2.

see that these spectral shifts are prominent at all frequencies on timescales when memory of the initial OH excitation frequency still exists ($\tau_2 = 250$ fs), much shorter than the structural relaxation of the liquid hydrogen-bond network (1–2 ps). Relaxation of these intertwined vibrations is marginally slower than the 200 fs OH···O hydrogen-bond stretching vibrational period, but short compared to the intermolecular motions. As early as 250 fs, the transient spectra resemble the equilibrium thermal difference spectrum even though the system is far from equilibrium. Thus we conclude that this observation is consistent with strong nonlinear coupling of the intermolecular hydrogen-bonding motions with the stretch and bend delocalized vibrations. This conclusion is consistent with recent theoretical studies that report strong coupling of stretch, bend and librational modes, in which bend excitation transfers between adjacent molecules in 50 fs, a timescale comparable to the period of bending vibrations (20 fs)[12].

Further information on the delocalized stretch–bend excitations was obtained from polarization-dependent transient absorption studies. Figure 4b shows the parallel and perpendicular dispersed transient absorption spectra of H_2O at 100 fs and 4 ps, and the calculated anisotropies at the bleach of the stretch (3,355 cm^{-1}) and bleach of the bend (1,670 cm^{-1}) detection frequencies are shown in Fig. 4e,f, respectively. From these spectra, it is clear that the stretch and induced absorption regions are polarized sharply. It seems that excitation of OH stretching motion polarizes charges along the constituent hydrogen bonds so that second OH excitation is enabled along the same orientation, although at much lower energy. The bleach has an anisotropy decay of 76 ± 14 fs at 3,355 cm^{-1}, which agrees with the measurements[9,19] and modelling[22] in the OH stretch region. The bend bleach, however, is depolarized from zero waiting time, which is consistent with the stretch being a delocalized excitation over several water molecules such that the orientation of the bend transition dipole is uncorrelated with that of the stretch.

Mechanism for vibrational coupling and energy dissipation. These results can be used to propose a molecular picture for energy relaxation and vibrations of the liquid. Infrared excitation of OH stretching transitions creates delocalized states with varying stretch and bend character. These excitons are by no means stationary and constantly evolve because of the motions of the liquid, which results in competing ultrafast energy transport and dissipation pathways. Depending on changing intermolecular configurations, it can transfer to configurations of lower energy within the exciton band, preferentially moving towards low-energy strongly hydrogen-bonded traps. Relaxation within the band guides the energy into resonance with the bend overtone, which makes it the preferred relaxation route. However, simultaneously we observe that direct energy relaxation to intermolecular motions acts to shift spectral bands at short times for the most strongly hydrogen-bonded OH oscillators. This is clear from the 2D IR spectra in Fig. 3a which shows a spectrally shifted band, highlighted by the asterisk, at $(\omega_1, \omega_3) = (3{,}200, 3{,}600)$ cm^{-1} for waiting times shorter than 250 fs. The stretch–bend exciton is coupled to the intermolecular degrees of freedom, which results in the response of the liquid on the timescales of the fastest intermolecular motions. Distributing the 3,400 cm^{-1} of energy among the large densities of stretch, bend and intermolecular modes therefore results in numerous channels for energy dissipation.

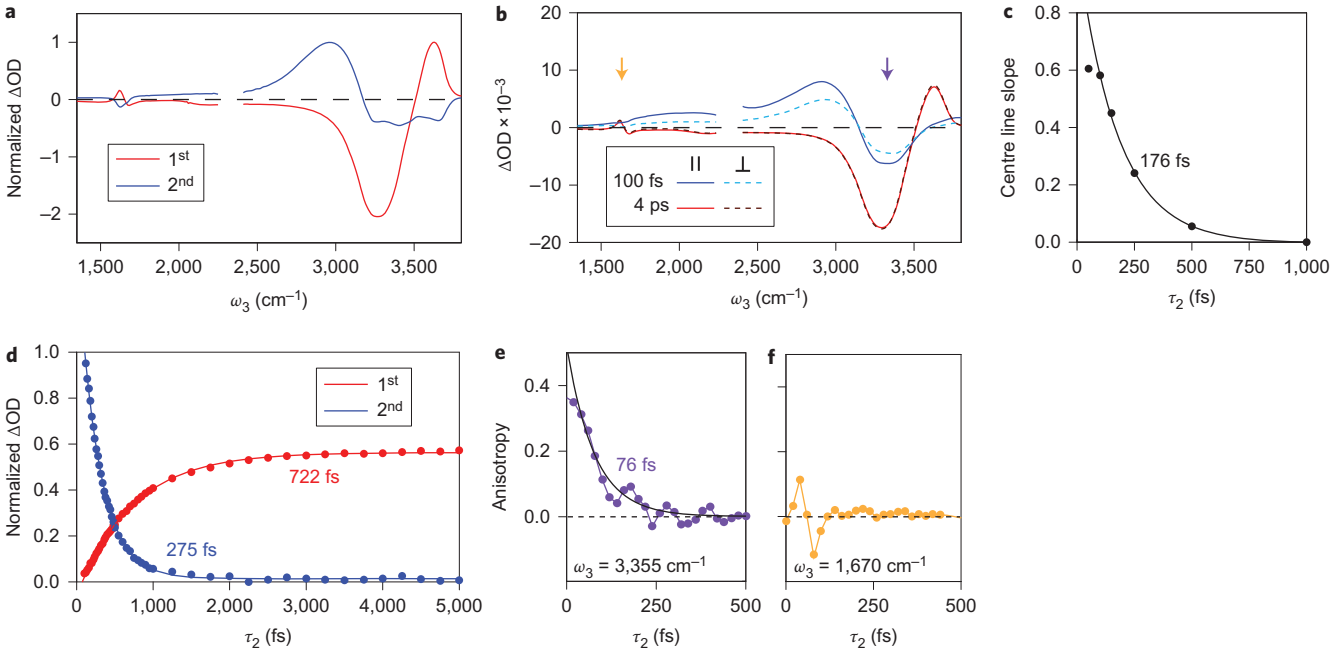

Figure 4 | Spectral and temporal analysis of ultrafast broadband infrared spectra of H_2O. a, The first two spectral components from a constrained SVD of the transient absorption spectrum from 100 fs to 5 ps. **b**, The parallel and perpendicular transient absorption spectra for waiting times of 100 fs and 4 ps. **c**, The centre line slope of the bleach in the OH stretching region of the broadband 2D IR spectra of H_2O as a function of waiting time. The decay was fit from 100 fs to 1 ps. The decay timescale was found to be 176±39 fs and the fit is shown as a black line. **d**, The temporal components that correspond to spectral components in **a**. The first component yielded a timescale of 722±16 fs, and the second component was fit to a timescale of 275±5 fs. Lines through the points are the fits. **e**, Time trace of pump–probe anisotropy for $\omega_3 = 3{,}355$ cm^{-1}, which decays on a 76 fs timescale. Fit is shown as a black line. **f**, The anisotropy of the bend calculated after correcting for the polarized induced-absorption offset.

Our proposal differs considerably from the traditional picture of vibrational relaxation, in which energy flows downhill through a set of weakly coupled intramolecular normal modes and into low-frequency collective intermolecular vibrations of the surroundings. This picture is commonly used to describe relaxation of the OH stretch excitation and the spectral shifting towards the thermal difference spectrum of water. In previous work it was concluded that OH stretch excitation flows into the overtone or the fundamental transition of the H_2O bend vibration, localized on one water molecule or across two neighbouring water molecules, and then into the collective motions of the liquid[3,8,10,11]. These pictures are appropriate in the case of weak coupling between donor and acceptor, when the timescale of energy exchange and relaxation exceeds the vibrational dephasing time. Although some previous studies recognized the existence of strong intermolecular coupling in water[3,15–17], vibrational energy relaxation is still conceived as an incoherent cascading downhill process. Excitonic models of the OH stretching vibration appear to capture its delocalization and intraband dynamics; however, we believe an accurate picture of the energy dissipation processes in water requires consideration of the mixing of stretch, bend and intermolecular motions.

Vibrations in water are coupled strongly enough that the local intermolecular configuration of the liquid dictates the form of the vibration. This observation suggests the presence of non-adiabatic effects that act to couple intra- and intermolecular motions strongly, an effect recently described in the 2D IR spectroscopy of isotopically dilute ice[23]. The rapid exchange of stretch and bend energy is also consistent with the concept of energy relaxation through vibrational 'conical intersections' in which the rapid non-adiabatic relaxation occurs through an intramolecular degeneracy that arises as a result of a particular intermolecular configuration[24].

Highly coupled and collective vibrational motions in water would have significant implications for the way in which we conceive of solutes in water and aqueous chemical reactivity. Traditional ways of thinking about the interaction between a solute and the solvating water molecules, in which their interaction is treated as a perturbation, may need to be re-evaluated for the case of aqueous solutes, especially when there is strong hydrogen bonding between the two. Given that water vibrations are delocalized, the vibrational eigenstates associated with the solute in water may also be delocalized, with correlations that extend over its solvation shell. The extent of coherent vibrational character of coupled solute and solvent also determines the distance scale and mechanism over which concerted bimolecular chemical reactions, such as proton transfer, can occur. These vibrational motions, in addition to dissipation, are also the origin of activation processes for solution-phase chemical reactions. Our results also imply that intermolecular motions can be coupled effectively to intramolecular modes of the system, which may act to funnel energy of collective motion and enhance local reactivity.

Methods

We used femtosecond broadband mid-infrared (BBIR) pulses that ranged in frequency from <400 cm^{-1} to 4,000 cm^{-1} for probing. These were generated with a laser plasma source, using the approach described by Petersen and Tokmakoff[25]. The BBIR was separated from the visible radiation by passing the beam through a sequence of gold mirrors and a 400 μm thick high-resistivity Si wafer placed at Brewster's angle. Generation of the 45 fs excitation pulses has been described previously[26]. Figure 1a shows the 3 μm and BBIR pulse spectra superimposed on the infrared spectrum of H_2O.

Broadband 2D IR experiments were done in the pump–probe geometry[27], in which the first two interactions are with collinear 3 μm excitation pulses, and the signal is measured as transient absorption changes on the BBIR probe. The 3 μm pulse pair for the 2D IR experiments was created by splitting the OPA output in a Mach–Zehnder interferometer. One of the two interferometer arms was sent to an interferometrically calibrated translation stage, and the other arm was chopped at half the laser repetition rate. The 3 μm pulses were delayed with respect to each other from −150 fs to 400 fs in steps of 2 fs to trace out the coherence oscillations in τ_1. These were subsequently numerically Fourier transformed to generate the ω_1 dimension of the 2D IR spectrum. The BBIR and the 3 μm beams were focused into

the sample using bare gold off-axis parabolic mirrors. The BBIR pulse was characterized temporally against the 45 fs 3 μm pulse using interferometric cross-correlation in a 50 μm pinhole. The envelope of the interferogram was fit to a Gaussian to yield a standard deviation of 70 fs and a BBIR pulse duration of <70 fs. An average positive chirp of ~70 fs over the 1,350–4,000 cm^{-1} region was characterized using non-resonant cross-correlation in a 1 mm thick CaF_2 window, dispersed on a HgCdTe array detector cooled by liquid nitrogen. The transient absorption spectra show the non-resonant response from the CaF_2 window, to some degree, around $\tau_2 = 0$.

For the broadband 2D IR spectra, the polarizations of pump and probe pulses were parallel. For transient absorption experiments, we rotated the polarization of the 3 μm beam relative to the BBIR using a λ/2 waveplate–wire-grid polarizer pair. The H_2O sample for these experiments was held between two 1 mm thick CaF_2 windows without a spacer, and the sample was maintained at room temperature. The optical density (OD) of the sample was kept between 0.8 and 1 at the peak of the OH stretch line shape at 3,400 cm^{-1} for both measurements. This corresponds to an OD of less than 0.3 at the 1,650 cm^{-1} H_2O bend transition.

After the sample, the transmitted BBIR probe was dispersed onto a 64-element HgCdTe array detector cooled by liquid nitrogen to generate the ω_3 dimension. The broadband 2D IR and transient absorption spectra were plotted from 1,500 cm^{-1} to 3,700 cm^{-1} and from 1,350 cm^{-1} to 4,000 cm^{-1}, respectively, where the low-frequency limit is imposed by the detector response. Four different positions of a 50 groove mm^{-1} grating were used to capture the BBIR spectrum from ~1,250 cm^{-1} to 4,200 cm^{-1}. To acquire data in the 4.5–7 μm region, we placed a long pass filter in front of the detector to eliminate artifacts associated with higher order dispersion from the grating. The entire set-up was enclosed in a box and purged with dry air to minimize atmospheric H_2O; however, atmospheric CO_2 at 4.25 μm caused distortions to the nonlinear spectra in that region.

Received 22 March 2013; accepted 14 August 2013; published online 22 September 2013

References

1. Pakoulev, A., Wang, Z. & Dlott, D. D. Vibrational relaxation and spectral evolution following ultrafast OH stretch excitation of water. *Chem. Phys. Lett.* **371,** 594–600 (2003).
2. Lindner, J., Cringus, D., Pshenichnikov, M. S. & Vöhringer, P. Anharmonic bend–stretch coupling in neat liquid water. *Chem. Phys.* **341,** 326–335 (2007).
3. Lindner, J. *et al.* Vibrational relaxation of pure liquid water. *Chem. Phys. Lett.* **421,** 329–333 (2006).
4. Wang, Z., Pakoulev, A., Pang, Y. & Dlott, D. D. Vibrational substructure in the OH stretching transition of water and HOD. *J. Phys. Chem. A* **108,** 9054–9063 (2004).
5. Larsen, O. F. A. & Woutersen, S. Vibrational relaxation of the H_2O bending mode in liquid water. *J. Chem. Phys.* **121,** 12143–12145 (2004).
6. Cowan, M. L. *et al.* Ultrafast memory loss and energy redistribution in the hydrogen bond network of liquid H_2O. *Nature* **434,** 199–202 (2005).
7. Huse, N., Ashihara, S., Nibbering, E. T. J. & Elsaesser, T. Ultrafast vibrational relaxation of O–H bending and librational excitations in liquid H_2O. *Chem. Phys. Lett.* **404,** 389–393 (2005).
8. Deàk, J. C., Rhea, S. T., Iwaki, L. K. & Dlott, D. D. Vibrational energy relaxation and spectral diffusion in water and deuterated water. *J. Phys. Chem. A* **104,** 4866–4875 (2000).
9. Kraemer, D. *et al.* Temperature dependence of the two-dimensional infrared spectrum of liquid H_2O. *Proc. Natl Acad. Sci. USA* **105,** 437–442 (2008).
10. Lock, A. J. & Bakker, H. J. Temperature dependence of vibrational relaxation in liquid H_2O. *J. Chem. Phys.* **117**, 1708–1713 (2002).
11. Ashihara, S., Huse, N., Espagne, A., Nibbering, E. T. J. & Elsaesser, T. Ultrafast structural dynamics of water induced by dissipation of vibrational energy. *J. Phys. Chem. A* **111,** 743–746 (2007).
12. Rey, R. & Hynes, J. T. Tracking energy transfer from excited to accepting modes: application to water bend vibrational relaxation. *Phys. Chem. Chem. Phys.* **14,** 6332–6342 (2012).
13. Jansen, T. L. C., Auer, B. M., Yang, M. & Skinner, J. L. Two-dimensional infrared spectroscopy and ultrafast anisotropy decay of water. *J. Chem. Phys.* **132,** 224503 (2010).
14. Yagasaki, T. & Saito, S. A novel method for analyzing energy relaxation in condensed phases using nonequilibrium molecular dynamics simulations: application to the energy relaxation of intermolecular motions in liquid water. *J. Chem. Phys.* **134,** 184503 (2011).
15. Auer, B. M. & Skinner, J. L. IR and Raman spectra of liquid water: theory and interpretation. *J. Chem. Phys.* **128,** 224511 (2008).
16. Paarmann, A., Hayashi, T., Mukamel, S. & Miller, R. J. D. Nonlinear response of vibrational excitons: simulating the two-dimensional infrared spectrum of liquid water. *J. Chem. Phys.* **130,** 204110 (2009).
17. Falvo, C., Palmieri, B. & Mukamel, S. Coherent infrared multidimensional spectra of the OH stretching band in liquid water simulated by direct nonlinear exciton propagation. *J. Chem. Phys.* **130,** 184501 (2009).
18. Hale, G. M. & Querry, M. R. Optical constants of water in the 200 nm to 200 μm wavelength region. *Appl. Opt.* **12,** 555–63 (1973).
19. Woutersen, S. & Bakker, H. J. Resonant intermolecular transfer of vibrational energy in liquid water. *Nature* **402,** 507–509 (1999).
20. De Marco, L., Ramasesha, K. & Tokmakoff, A. Experimental evidence for Fermi resonances in isotopically dilute water from ultrafast IR spectroscopy. *J. Phys. Chem. B* doi:10.1021/jp4034613 (2013).
21. Libnau, F. O., Kvalheim, O. M., Christy, A. A. & Toft, J. Spectra of water in the near- and mid-infrared region. *Vib. Spec.* **7,** 243–254 (1994).
22. Yang, M., Li, F. & Skinner, J. L. Vibrational energy transfer and anisotropy decay in liquid water: is the Förster model valid? *J. Chem. Phys.* **135,** 164505 (2011).
23. Perakis, F., Widmer, S. & Hamm, P. Two-dimensional infrared spectroscopy of isotope-diluted ice Ih. *J. Chem. Phys.* **134,** 204505 (2011).
24. Hamm, P. & Stock, G. Vibrational conical intersections as a mechanism of ultrafast vibrational relaxation. *Phys. Rev. Lett.* **109,** 1–5 (2012).
25. Petersen, P. B. & Tokmakoff, A. Source for ultrafast continuum infrared and terahertz radiation. *Opt. Lett.* **35,** 1962–1964 (2010).
26. Fecko, C. J., Loparo, J. J. & Tokmakoff, A. Generation of 45 femtosecond pulses at 3 μm with a KNbO optical parametric amplifier. *Opt. Commun.* **241,** 521–528 (2004).
27. Deflores, L. P., Nicodemus, R. A. & Tokmakoff, A. Two-dimensional Fourier transform spectroscopy in the pump–probe geometry. *Opt. Lett.* **32,** 2966–2968 (2007).

Acknowledgements

This work was supported by the US Department of Energy (DE-FG02-99ER14988). L.D.M thanks the Natural Sciences and Engineering Research Council of Canada for a scholarship.

Author contributions

A.T., K.R. and L.D.M. conceived and designed experiments. K.R., L.D.M. and A.M. constructed the spectrometer and performed the experiments. A.T., K.R., L.D.M. and A.M. analysed results. K.R. and A.T. co-wrote the paper.

Additional information

Reprints and permissions information is available online at www.nature.com/reprints. Correspondence and requests for materials should be addressed to A.T.

Competing financial interests

The authors declare no competing financial interests.